

# On Absorbing Boundary Conditions for Wave Propagation<sup>1</sup>

A. BARRY,\* J. BIELAK,\* AND R. C. MACCAMY†

*\*Department of Civil Engineering and †Department of Mathematics,  
Carnegie-Mellon University, Pittsburgh, Pennsylvania 15213*

Received June 26, 1987; revised March 25, 1988

This paper is concerned with the development of methods for constructing stable artificial boundary conditions for wavelike equations in a general and automatic way. The one-dimensional problem of a semi-infinite, inhomogeneous, elastic bar is studied here as a prototype situation. For this problem a family of efficient artificial boundary conditions is obtained using geometrical optics in the Laplace transform domain for generating outgoing solutions, together with a stability criterion based on energy integrals to insure that the resulting artificial boundaries are dissipative. Numerical examples illustrate the efficacy of this approach. The paper also includes some remarks about the extension of the proposed method to a more general two-dimensional situation. © 1988 Academic Press, Inc.

## 1. INTRODUCTION

The method of artificial boundaries is a device to obtain approximate solutions of differential equation problems in infinite domains. It involves introducing an artificial boundary and giving approximate boundary conditions. Then one can solve a problem in a finite domain.

The method has been used by many authors (see, e.g., the survey by Turkel [11]). Our ideas were influenced particularly by the systematic and ingenious work of Engquist and Majda [4] and [5]. They gave a very complete discussion of the exterior problem for the wave equation in a half-space. This problem had the advantage that much of the work could be done with explicit formulas. We had some difficulty, however, in understanding how the method would work in more general situations. To aid us in this respect, we undertook a study of the one-dimensional problem of a semi-infinite, inhomogeneous, elastic bar. We report our observations here.

Our first step was to use geometrical optics ideas in the Laplace transform domain to develop a sequence of approximate problems. This seems to provide a straightforward and systematic procedure for doing the pseudodifferential operator factoring of [4] and [5], and generating outgoing solutions. Related ideas appear in [7-9].

<sup>1</sup>This work was supported by the National Science Foundation under Grants ECE-86/1060 (J.B., A.B.) and DMS 8601288 (R.C.M.).

The approximate problems can be solved easily with finite element methods. When we implemented them, however, we observed exponential error growth. This is to be anticipated from the work of [4] and [5], since our artificial conditions violate the well-posedness criterion given there. Thus one must somehow modify the artificial conditions.

In order to produce stable solutions we developed a criterion for stability that makes use of energy integrals, and is thus fairly general. Finally, we obtained a very simple modification of our approximate conditions which satisfies our criterion for stability. These modified conditions, which are as easy to implement as our original ones, produced a dramatic improvement in accuracy. Numerical examples are given in Section 4 to illustrate this effect.

We believe that the above ideas have considerable generality. As an illustration, in Section 5 we make some remarks on the much more difficult case of two-dimensional problems. In particular, we consider the exterior wave equation problem. We follow the same sequence of steps: geometrical optics expansion in the transform domain and development of a stability criterion via energy integrals. We are able to treat the problem of a general convex artificial boundary in a systematic way but we encounter the difficulty that the approximate problems do not satisfy our stability criterion. Again, this is anticipated by the work of [4] and [5]. For the half-space problem this difficulty was overcome in [4] and [5] by a clever use of Padé approximations. We do not see, however, how to extend the Padé approach to the general case.

For the general case we propose a modified condition that we hope will partially overcome the stability problem. We also indicate in Section 5 a connection between our work and that of Bayliss and Turkel [2] when we choose our two-dimensional boundary to be a circle.

Our main goal was to obtain methods for construction of artificial boundary conditions and stability criteria which are both general and automatic. We feel that the geometrical optics and energy integral arguments are vehicles to this end.

## 2. ANALYSIS OF THE BAR PROBLEM

We treat the problem of a semi-infinite elastic bar, of uniform cross section, under impact. The bar is inhomogeneous in the axial direction and the motion is assumed to be purely longitudinal.

Let  $x$  denote position of the cross sections in the unstretched configuration and let  $u(x, t)$ ,  $\rho(x)$ , and  $\mu(x)$  denote displacement, density, and elastic modulus. The stress  $\sigma(x, t) = \mu(x) u_x(x, t)$  and the mathematical problem, which we denote by (P), is

$$\begin{aligned} \rho(x) u_{tt}(x, t) &= \sigma_x(x, t) = (\mu(x) u_x(x, t))_x, & x > 0, \quad t > 0; \\ \sigma(0, t) &= \mu(0) u_x(0, t) = \psi(t), & t > 0; \\ u(x, 0) &\equiv u_t(x, 0) \equiv 0, & x > 0 \end{aligned} \tag{2.1}$$

We assume that the bar is eventually homogeneous, that is,

$$\rho(x) \equiv \rho_0, \quad \mu(x) \equiv \mu_0 \quad \text{for } x \geq \bar{x}$$

and we require the solution to be *outgoing*, that is,

$$\sigma(x, t) = \mu_0 u_x(x, t) = -\sqrt{\rho_0 \mu_0} u_t(x, t) \quad \text{for } x \geq \bar{x}. \tag{2.2}$$

It would be quite straightforward to solve (P) on  $(0, \bar{x})$ , with condition (2.2) at  $x = \bar{x}$ , by finite element or finite difference methods. If  $\bar{x}$  is large, however, this would lead to large systems of algebraic equations. Further, one may be interested in  $u$  only for values of  $x$  close to zero. Thus the question arises as to whether one can solve (P) over a shorter interval  $(0, L)$  with some approximate boundary condition at  $x = L$ .

We begin our analysis by Laplace transforming (2.1) with respect to time. This yields the problem

$$\begin{aligned} \rho s^2 \hat{u}(x, s) &= (\mu(x) \hat{u}_x(x, s))_x, & x > 0, \\ \hat{\sigma}(0, s) &= \mu(0) \hat{u}_x(0, s) = \hat{\psi}(s). \end{aligned} \tag{2.3}$$

The outgoing condition (2.2) requires that  $\hat{u}$  satisfy

$$\hat{\sigma}(x, s) = \mu_0 \hat{u}_x(x, s) = -\sqrt{\rho_0 \mu_0} s \hat{u}(x, s), \quad x \geq \bar{x}. \tag{2.4}$$

Suppose that  $\hat{U}(x, s)$  is a solution of the problem

$$\begin{aligned} \rho s^2 \hat{U}(x, s) &= (\mu(x) \hat{U}_x(x, s))_x, & x > L, \\ \hat{U}(L, s) &= 1, \quad \mu_0 \hat{U}_x(L, s) = -\sqrt{\rho_0 \mu_0} s \hat{U}(L, s), & x \geq \bar{x}. \end{aligned} \tag{2.5}$$

Then one has  $\hat{u}(x, s) = \hat{u}(L, s) \hat{U}(x, s)$  on  $x \geq L$ . Hence we have

$$\hat{\sigma}(L, s) = \mu(L) \hat{u}_x(L, s) = \mu(L) \hat{U}_x(L, s) \hat{u}(L, s) \equiv \hat{\mathcal{F}}(s) \hat{u}(L, s). \tag{2.6}$$

Equation (2.6) represents an exact boundary condition satisfied by the solution of (2.3). Translated back into the time domain it gives

$$\sigma(L, t) = \mathcal{F}(u'(L, \cdot)), \tag{2.7}$$

where  $u'$  represents the history,  $u'(L, t) = u(L, t - \tau)$ . If one solved the problem

$$\begin{aligned} \rho u_{tt} &= (\mu u_x)_x, & u(x, 0) = u_t(x, 0) &= 0, & 0 < x < L, \\ \sigma(0, t) &= \psi(t), & \sigma(L, t) &= \mathcal{F}(u'(L, \cdot)), \end{aligned} \tag{2.8}$$

one would have the exact solution of (2.1) on  $(0, L)$ .

The quantity  $\hat{\mathcal{F}}$  and hence the operator  $\mathcal{F}$  is hard to compute. Even if it were known condition (2.7) would cause numerical difficulty since it is non-local in time.

Our goal is to obtain approximations to  $\hat{\mathcal{F}}$ , hence  $\mathcal{F}$ , which are easier to use.  $\mathcal{F}$  is a pseudodifferential operator and it is the operator  $R(t)$  in [7, Sect. 4]. It is indicated in [7] that one can approximate  $R(t)$  for highly oscillatory functions by analyzing its transform for large  $s$ . The same approach is suggested by the work of [8]. We will carry out this approach in a systematic fashion by using ideas from geometrical optics (see, e.g., [3]).

Our procedure is to seek an asymptotic expansion for the function  $\hat{U}$  in (2.5) for large  $s$ . This expansion has the form

$$\begin{aligned} \hat{U}(x, s) &\sim e^{-s\phi(x)} \sum_{k=0}^{\infty} U_k(x) s^{-k}, \\ \phi(L) &= 0, \quad U_0(L) = 1, \quad U_k(L) = 0, \quad k \geq 1. \end{aligned} \tag{2.9}$$

We substitute (2.9) into (2.5) and equate coefficients of  $s^{-k}$ . This yields, first, the equation

$$\phi'(x) = \sqrt{\rho(x)/\mu(x)}. \tag{2.10}$$

The  $U_k$ 's are then determined recursively. If we put  $\beta(x) = \sqrt{\rho(x)\mu(x)}$  then

$$2\beta U'_0 + \beta' U_0 = 0, \quad 2\beta U'_k + \beta' U_k = (\mu U'_{k-1})', \quad k \geq 1. \tag{2.11}$$

We obtain an expansion for  $\hat{\mathcal{F}}(s)$  by differentiating (2.9) and setting  $x=L$  to obtain

$$\begin{aligned} \hat{\mathcal{F}}(s) &= \mu(L) \hat{U}_x(L, s) \sim \mu(L) \\ &\times \left\{ -s\phi'(L) + \sum_{k=0}^{\infty} U'_L(L) s^{-k} \right\} = \sum_{k=-1}^{\infty} \alpha_k s^{-k}. \end{aligned} \tag{2.12}$$

The coefficients  $\alpha_k$  are computed from (2.11) at  $x=L$  and are determined by  $\rho$  and  $\mu$  and their derivatives at  $x=L$ . We record the first three coefficients in the case  $\rho(x) \equiv 1$ , which was that used in our numerical experiments:

$$\begin{aligned} \alpha_{-1} &= -\sqrt{\mu(L)}, \quad \alpha_0 = -\frac{1}{4} \mu'(L), \\ \alpha_1 &= \frac{\sqrt{\mu(L)}}{8} \left\{ -\mu''(L) + \frac{1}{4} \frac{\mu'(L)^2}{\mu(L)} \right\}. \end{aligned} \tag{2.13}$$

One can obtain approximate boundary conditions by truncating the series (2.12). Thus we define  $\hat{\mathcal{F}}'_N(s)$  by the formulas

$$\hat{\mathcal{F}}'_N(s) = \sum_{k=-1}^N \alpha_k s^{-k} \tag{2.14}$$

and replace condition (2.6) by  $\hat{\sigma}(L, s) = \hat{\mathcal{F}}'_N(s) \hat{u}(L, s)$ . We note that if  $\varphi_k(t) = ((k-1)!)^{-1} t^{k-1}$ ,  $k = 1, 2, \dots$ , then  $\hat{\varphi}^k(s) = s^{-k}$ . Thus (2.14) corresponds in the time domain to the approximate boundary conditions

$$\sigma(L, t) = \mathcal{F}'_N(u'(L, \cdot)) = \alpha_{-1} u_t(L, t) + \alpha_0 u(L, t) + \sum_{k=1}^N \alpha_k (\varphi_k * u(L, \cdot))(t) \tag{2.15}$$

where  $(*)$  denotes convolution. We note that the integrals can be eliminated. There are polynomials  $P_N(z)$  and  $Q_N(z)$  such that (2.15) is the same as

$$P_N(D) \sigma(L, t) = Q_N(D) u(L, t), \quad D = \frac{\partial}{\partial t}. \tag{2.16}$$

For  $N = -1, 0, 1$  we have, respectively,

$$\sigma(L, t) = \alpha_{-1} u_t(L, t), \tag{2.17a}$$

$$\sigma(L, t) = \alpha_{-1} u_t(L, t) + \alpha_0 u(L, t), \tag{2.17b}$$

$$\sigma_t(L, t) = \alpha_{-1} u_{tt}(L, t) + \alpha_0 u_t(L, t) + \alpha_1 u(L, t). \tag{2.17c}$$

*Remarks.* (1) If  $\rho$  and  $\mu$  were constants  $\rho_0$  and  $\mu_0$  series (2.9) would reduce to a single term  $\hat{U}(x, s) = e^{-s\phi(x)}$ ,  $\phi(x) = \sqrt{\rho_0\mu_0}(x-L)$  and then  $\alpha_{-1} = -\sqrt{\rho_0\mu_0}$ ,  $\alpha_k = 0$  for  $k \geq 0$ . Thus the  $\hat{\mathcal{F}}'_N$ 's are all equal to the exact  $\hat{\mathcal{F}}$ .

(2) Suppose one truncates series (2.9) at  $k = N$  to obtain functions  $\hat{U}^N(x, s)$ . It is easy to verify that these solve the problems

$$\begin{aligned} \rho s^2 \hat{U}^N(x, s) &= (\mu(x) \hat{U}_x^N(x, s)) + f^N(x, s), \\ U^N(L, s) &= 1, \quad \mu_0 U_x^N(x, s) = -\sqrt{\rho_0\mu_0} s U^N(x, s), \quad x \geq \bar{x}, \end{aligned}$$

where  $f^N(x, s) = O(s^{-N})$ . From this it is possible to show that (2.9) is indeed an asymptotic expansion in the sense that  $\hat{U} - \hat{U}^N = O(s^{-N-1})$  for large  $s$ . The same is true for the approximate  $\hat{\mathcal{F}}$  in (2.14).

(3) It is of interest to note that one can also obtain an expansion for  $\hat{U}(s)$  and hence  $\hat{\mathcal{F}}(s)$  for small  $s$ . Thus one could take

$$\hat{U}(x, s) = \sum_{k=0}^{\infty} V_k(x) s^k. \tag{2.18}$$

If one substitutes into (2.5) one obtains

$$V_0(x) \equiv 1, \quad V_1(x) = -\sqrt{\rho_0\mu_0} \int_L^x \mu(\xi)^{-1} d\xi. \tag{2.19}$$

It follows that for small  $s$   $\hat{\mathcal{F}}(s)$  has an expansion

$$\hat{\mathcal{F}}(s) = \sum_{k=1}^{\infty} \beta_k s^k, \quad \beta_1 = -\sqrt{\rho_0 \mu_0}. \tag{2.20}$$

Note in particular that  $\hat{\mathcal{F}}(0) = 0$ . From (2.20) one can obtain a different set of approximate boundary conditions corresponding to  $\hat{\mathcal{F}}_N''(s) = \sum_{k=1}^N \beta_k s^k$ , that is,

$$\sigma(L, t) = \sum_{k=1}^{\infty} \beta_k D^k u(L, t), \quad D = \frac{\partial}{\partial t}. \tag{2.21}$$

We have not studied condition (2.21) numerically.

Let us return to conditions (2.16). The problems  $(P'_N)$  which one would solve numerically are

$$\begin{aligned} \rho u_{tt} &= (\mu u_x)_x, & u(x, 0) &= u_t(x, 0) = 0, & 0 < x < L, \\ \sigma(0, t) &= \psi(t), & P_N(D) \sigma(L, t) &= Q_N(D) u(L, t). \end{aligned} \tag{2.22}$$

Our numerical procedure, as described in Section 4, is a mixed finite element variational method, with  $u(x, t)$  and  $\sigma(L, t)$  as variables. Conditions (2.16) are easy to implement within this framework and we feel the method extends to other situations more easily than finite differences.

The hope is that if one solves (2.22) for  $u^N$  then  $u^N$  will approximate the solution  $u$  of (2.1) on  $(0, L)$  with increasing accuracy as  $N$  increases. (For a fixed  $N$  the accuracy should increase as  $L$  increases, with the solution becoming exact as  $L \rightarrow \bar{x}$ .) The results of some numerical experiments are presented in Section 4. We found that the cases  $N = -1$  and  $0$  work fairly well, even for small  $L$ , with  $N = 0$ , in general, better than  $N = -1$ . For  $N = 1$ , however, we observed errors which grow rapidly as  $t$  increases. We want to discuss this now and provide a modification which reduces the errors.

It has been observed in studying artificial boundary conditions that one must be careful that these conditions do not produce ill-posed problems. The criterion used in [4] and [5] for acceptable approximate conditions is that of Kreiss [10]. In the simple situation we are considering it amounts to the following. Consider the equation  $\rho(L) u_{tt} = \mu(L) u_{xx}$ . Then a boundary condition at  $x = L$  is well posed in the sense of Kreiss if there is no solution  $u(x, t) = e^{sx + \lambda t}$ , satisfying that condition, for  $\Re s > 0$ . One verifies immediately that this will be true for boundary condition (2.17) if and only if the constants  $\alpha_{-1}$ ,  $\alpha_0$ , and  $\alpha_1$  are all negative. In our experiments we chose a  $\mu$  which is monotone increasing but concave. Thus we see from (2.13) that  $\alpha_{-1} < 0$  and  $\alpha_0 < 0$  but  $\alpha_1 > 0$ . Thus our condition (2.17c) for  $N = 1$  is ill posed according to the Kreiss criterion.

We introduce a more restrictive stability criterion for the approximate condition at  $x = L$ . We term this *dissipativity*. The goal is to prevent exponential error growth with time. Our condition appears naturally from energy integral arguments, is satisfied by the exact operator  $\mathcal{F}$  of (2.7), and is easy to check.

Let  $\mathcal{S}$  denote a history operator of the type considered above and let  $\hat{\mathcal{S}}$  denote its Laplace transform. We consider the problem  $\mathcal{P}(\mathcal{S}, \psi, \chi)$ ,

$$\begin{aligned} \rho u_{tt} &= (\mu u_x)_x, & u(x, 0) &= u_x(x, 0) = 0, & 0 < x < L, \\ \sigma(0, t) &= \mu(0) u_x(0, t) = \psi(t), & & & (2.23) \\ \sigma(L, t) - \mathcal{S}(u'(L, \cdot)) &= \mu(L) u_x(L, t) - \mathcal{S}(u'(L, \cdot)) = \chi(t), \end{aligned}$$

and its transform  $\hat{\mathcal{P}}(\hat{\mathcal{S}}, \hat{\psi}, \hat{\chi})$ ,

$$\begin{aligned} \rho s^2 \hat{u} &= (\mu \hat{u}_x)_x, & 0 < x < L, \\ \hat{\sigma}(0, s) &= \hat{\psi}(s), & \hat{\sigma}(L, s) &= \mu(L) \hat{u}_x(L, s) = \hat{\mathcal{S}}(s) \hat{u}(L, s) + \hat{\chi}. \end{aligned} \tag{2.24}$$

DEFINITION.  $\mathcal{S}$  is *dissipative* if  $\hat{\mathcal{P}}(\hat{\mathcal{S}}, 0, 0)$  has no non-zero solutions for  $s \neq 0$ ,  $\Re s \geq 0$ .

Remark 4. Observe that if  $\mathcal{S}(0)$  is zero then for  $s = 0$  (2.24) will have constant solutions for  $\hat{\chi} \equiv 0$ . We observed above that the  $\hat{\mathcal{F}}$  in (2.6) is zero when  $s = 0$ ; thus we have excluded  $s = 0$  in the definition of dissipativity.

Let us indicate the implications of this condition. Suppose that the data  $\psi$  and  $\chi$  are such that their transforms  $\hat{\psi}, \hat{\chi}$  are analytic in  $\Re s \geq 0$ . Then one has the following results:

- (i) If  $\mathcal{S}$  is dissipative the solution  $\hat{u}$  of  $\mathcal{P}(\mathcal{S}, \hat{\psi}, \hat{\chi})$  will exist and be continuous in  $\Re s \geq 0, s \neq 0$ , and analytic in  $\Re s > 0$ .
- (ii) If  $\mathcal{S}$  is not dissipative then the solution  $\hat{u}$  of  $\mathcal{P}(\mathcal{S}, \hat{\psi}, \hat{\chi})$  will (in general) have poles in  $\Re s > 0$ .

One recovers  $u$  by taking the inverse transform of  $\hat{u}$ . Thus if  $\mathcal{S}$  is not dissipative (ii) implies that  $u$  will usually grow exponentially with time. If  $\mathcal{S}$  is dissipative (i) implies this cannot happen and, in general, one would expect  $u$  to remain bounded as  $t$  tends to infinity.

We will show that  $\mathcal{F}$  in (2.7) is dissipative. Suppose we can find an approximating operator  $\mathcal{F}'$  which is also dissipative. Let  $u$  be the exact solution of (2.1), that is,  $\mathcal{P}(\mathcal{F}, \psi, 0)$  and let  $v$  be the solution of the approximating problem  $\mathcal{P}(\mathcal{F}', \psi, 0)$ . Then the error  $w = u - v$  will be a solution of  $\mathcal{P}(\mathcal{F}, 0, \chi)$  with  $\chi(t) = \mathcal{F}[u'(L, \cdot)] - \mathcal{F}'[u'(L, \cdot)]$ . Thus the dissipativity of  $\mathcal{F}'$  will prevent exponential error growth.

We give sufficient conditions for dissipativity.

PROPOSITION 1.  $\mathcal{S}$  is dissipative if  $\hat{\mathcal{S}}$  satisfies the two conditions

$$\begin{aligned} \hat{\mathcal{S}}(s) &< 0 & \text{for any } s = \xi, & \xi > 0, & (\hat{R}) \\ \Im \hat{\mathcal{S}}(\xi + i\eta) &\begin{cases} < 0 \\ > 0 \end{cases} & \text{for any } \xi + i\eta & \text{with } \xi \geq 0 \text{ and } \begin{cases} \eta > 0, \\ \eta < 0. \end{cases} & (\hat{I}) \end{aligned}$$

*Proof.* Let  $u$  be a solution of  $\mathcal{P}(\mathcal{S}, 0, 0)$  so that  $\hat{u}$  is a solution of  $\hat{\mathcal{P}}(\hat{\mathcal{S}}, 0, 0)$ . Then from (2.24) we have

$$0 = s^2 \int_0^L \rho(x) |\hat{u}(x, s)|^2 dx + \int_0^L \mu(x) |\hat{u}_x(x, s)|^2 dx - \hat{\mathcal{P}}(s) |\hat{u}(L, s)|^2. \tag{2.25}$$

For  $s = \xi > 0$  (2.25) and  $(\hat{R})$  imply  $\hat{u}(x, s) \equiv 0$ . For  $s = \xi + i\eta$ ,  $\xi > 0$ ,  $\eta \neq 0$ . For  $s = i\eta$ ,  $\eta \neq 0$ , we take the imaginary part of (2.25) and use  $(\hat{I})$  to conclude  $\hat{u}(L, S) = 0$ . But then we have also  $\hat{u}_x(L, S) = \mathcal{S}(s) \hat{u}(L, S) = 0$  and hence  $\hat{u}(x, s) \equiv 0$  by unique continuation.

We use  $(\hat{R})$  and  $(\hat{I})$  to show that  $\mathcal{F}$  in (2.7) is dissipative.

**PROPOSITION 2.** *The operator  $\mathcal{F}$  in (2.7) is dissipative.*

*Proof.* From (2.5) we have  $(\hat{U}(L, S) = 1)$ ,

$$\begin{aligned} 0 = s^2 \int_L^{\bar{x}} \rho(x) |\hat{U}(x, s)|^2 dx + \int_L^{\bar{x}} \rho(x) |\hat{U}_x(x, s)|^2 dx \\ + \sqrt{\rho_0 \mu_0} s |\hat{U}(\bar{x}, s)|^2 + \mathcal{F}(s) |U(L, s)|^2. \end{aligned} \tag{2.26}$$

We note that  $\hat{U}(\bar{x}, s)$  cannot be zero. If it were we would have  $\hat{U}_x(\bar{x}, s) = 0$  also and, as above,  $\hat{U}(x, s) \equiv 0$ . Then for  $s = \xi > 0$   $(\hat{R})$  follows from (2.26) and, for  $s = \xi + i\eta$ ,  $\xi \geq 0$ ,  $\eta \neq 0$   $(\hat{I})$  follows by taking the imaginary part of (2.26).

Let us consider our approximate operator  $\mathcal{F}'_1(s) = \alpha_{-1}s + \alpha_0 + \alpha_1 s^{-1}$  and suppose  $\alpha_{-1} < 0$  and  $\alpha_0 < 0$ . Then if  $\alpha_1 > 0$   $(\hat{R})$  will be violated. (Recall this is the case we studied numerically.) If  $\alpha_1$  were negative we would violate  $(\hat{I})$  thus with  $\alpha_{-1} < 0$  and  $\alpha_0 < 0$  our  $\mathcal{F}'_1$  could never be dissipative.

We observed that one can satisfy both  $(\hat{R})$  and  $(\hat{I})$  with a simple modification of  $\mathcal{F}'_1$ ; namely, one takes

$$\hat{\mathcal{F}}_1(s) = \alpha_{-1}s + \alpha_0 + \alpha_1(s + \delta)^{-1}. \tag{2.27}$$

For any  $\delta$   $\hat{\mathcal{F}}(s)$  will agree with  $\hat{\mathcal{F}}'_1(s)$  to order  $s^{-2}$  for large  $s$ . With  $\alpha_{-1} < 0$  and  $\alpha_0 < 0$  we see that when  $\alpha_1 > 0$   $\mathcal{F}_1$  is dissipative if  $\delta > -\alpha_1/\alpha_0$  while if  $\alpha_1 < 0$  it is dissipative for  $\delta > (\alpha_1/\alpha_{-1})^{1/2}$ .

When we use the revised operator  $\mathcal{F}_1$  the problem  $(P'_1)$  in (2.22) is replaced by problem  $(P_1)$ :

$$\begin{aligned} \rho u_{tt} = (\mu u_x)_x, \quad u(x, 0) = u_t(x, 0) = 0, \quad 0 < x < L, \\ \sigma_t(L, t) + \delta \sigma(L, t) = \alpha_{-1} u_{tt}(L, t) + (\alpha_0 + \alpha_{-1} \delta) u_t(L, t) \\ + (\alpha_1 + \alpha_0 \delta) u(L, t). \end{aligned} \tag{2.28}$$



This problem is as easy to implement numerically as  $(P'_1)$  and, as we show in Section 4, it produces dramatically reduced errors.

*Remarks.* (5) The modification (2.27) appears to be related to one suggested in Eq. (3.13) of [9] but the relation is not clear.

(6) Our modification can be extended to the higher order operators  $\mathcal{F}'_N$ , namely, one can introduce  $\hat{\mathcal{F}}_N$  defined by

$$\hat{\mathcal{F}}_N(s) = \alpha_{-1}s + \alpha_0 + \sum_{k=1}^N \alpha_{k,N}(s + \delta_{k,N})^{-k}. \tag{2.29}$$

One can choose the constants  $\alpha_{k,N}$  and  $\delta_{k,N}$  so that  $\hat{\mathcal{F}}_N$  agrees with  $\mathcal{F}'_N$  up to order  $s^{-N-1}$  while  $\hat{\mathcal{F}}_N$  is dissipative. (This is again similar to Ref. [9].) Condition (2.29) translated back to the time domain again yields problems like (2.23). Some preliminary calculations for  $N=2$  indicated a slight improvement but also exhibited some numerical instabilities due to the higher order time derivatives. Thus it is not clear that it would be desirable to use higher order approximations.

(7) Our approximate boundary conditions have an interesting mechanical interpretation. Condition (2.17a) could be realized by attaching a dashpot of constant  $-\alpha_{-1}$  to the end  $x=L$  of a finite bar. Condition (2.17b) is the same as attaching a dashpot, with constant  $-\alpha_{-1}$ , and a spring, with constant  $-\alpha_0$ , in parallel. The modified condition in (2.28) could be realized by the arrangement of springs and dashpots indicated in Fig. 1.

It can be checked that this yields the desired condition, for a given  $\delta > 0$ , provided we choose the spring constants  $k_i$  and dashpot constants  $c_i$  by

$$c_0 = -\alpha_{-1}, \quad k_1 = \alpha_1/\delta, \quad k_0 = -\alpha_0 - \alpha_1/\delta, \quad c_1 = k_1/\delta. \tag{2.30}$$

We assume, as in our numerical example, that  $\alpha_{-1} < 0$ ,  $\alpha_0 < 0$ , and  $\alpha_1 > 0$ . Thus the system is physically realizable (all constants positive) precisely when  $\delta > \alpha_1/-\alpha_0$ , which is our stability condition. We note that for the unmodified condition (2.17c), for  $N=1$ , it is not possible to have a physically realizable equivalent spring-dashpot system.

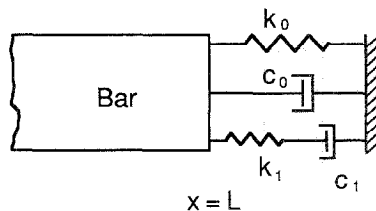


FIG. 1. Mechanical representation of modified absorbing boundary condition in (2.28).

3. NUMERICAL IMPLEMENTATION

We solved problems (2.22) and (2.28) by a variational procedure using finite elements. We illustrate with (2.28). If one puts  $\tau(t) = \sigma(L, t)$  one has the following mixed variational form: Find  $u(x, t)$  and  $\tau(t)$  such that for any differentiable  $v(x)$ ,

$$\int_0^L [\rho(x) u_{tt}(x, t) v(x) + \mu(x) u_x(x, t) v'(x)] dx - \tau(t) v(L) = -\psi(t) v(0),$$

$$\dot{\tau}(t) + \delta\tau(t) = \alpha_{-1} u_{tt}(L, t) + \kappa_0 u_t(L, t) + \kappa_1 u(L, t), \tag{3.1}$$

$$\kappa_0 = \alpha_0 + \alpha_{-1} \delta, \quad \kappa_1 = \alpha_1 + \alpha_0 \delta.$$

We introduce the finite-dimensional spaces  $S^h$  spanned by the piecewise linear finite elements  $\varphi_k^h$ . Then we seek

$$u^h(x, t) = \sum_0^{N_h} u_k^h(t) \varphi_k^h(x)$$

which satisfy (3.1) for all  $u \in S^h$ . The resulting spatially discretized problems can be reduced to the form

$$\mathbf{M}\ddot{\mathbf{u}}(t) + \mathbf{K}\mathbf{u}(t) - \tau(t) \mathbf{e}_{N_h} = -\psi(t) \mathbf{e}_0, \quad \mathbf{u}(0) = \dot{\mathbf{u}}(0) = 0,$$

$$\dot{\tau}(t) + \delta\tau(t) = \alpha_{-1} \ddot{u}_{N_h} + \kappa_0 \dot{u}_{N_h} + \kappa_1 u_{N_h}, \quad \tau(0) = 0. \tag{3.2}$$

For the time integration of (3.2), we used Newmark's trapezoidal method [6]. At the time step  $(r + 1)$ , (3.2) is written as

$$\mathbf{M}\ddot{\mathbf{u}}^{r+1} + \mathbf{K}\mathbf{u}^{r+1} - \tau^{r+1} \mathbf{e}_{N_h} = -\psi^{r+1} \mathbf{e}_0. \tag{3.3}$$

The displacements  $\mathbf{u}^{r+1}$  and velocities  $\dot{\mathbf{u}}^{r+1}$  are obtained as

$$\mathbf{u}^{r+1} = \dot{\mathbf{u}}^r + \dot{\mathbf{u}}^r \Delta t + (\ddot{\mathbf{u}}^r + \ddot{\mathbf{u}}^{r+1})(\Delta t)^2/4,$$

$$\dot{\mathbf{u}}^{r+1} = \dot{\mathbf{u}}^r + (\ddot{\mathbf{u}}^r + \ddot{\mathbf{u}}^{r+1}) \Delta t/2. \tag{3.4}$$

For a prescribed  $\tau$  this algorithm is unconditionally stable [6]. The time integration of (3.2)<sub>3</sub> is carried out by a backward difference scheme combined with averaging,

$$(\tau^{r+1} - \tau^r)/\Delta t + \frac{\delta}{2} (\tau^{r+1} + \tau^r) = \alpha_{-1} (\dot{u}_{N_h}^{r+1} - \dot{u}_{N_h}^r)/\Delta t$$

$$+ \kappa_0 (u_{N_h}^{r+1} - u_{N_h}^r)/\Delta t + \frac{\kappa_1}{2} (u_{N_h}^{r+1} + u_{N_h}^r). \tag{3.5}$$

*Remark.* The use of the mixed variational procedure, with  $\mu(L) u_x(L, t)$  as an unknown eliminates the necessity for calculating the  $x$  derivative of  $u$  at  $x = L$ . This seems preferable to finite differences.

4. NUMERICAL RESULTS

To illustrate the applicability of our procedure we consider a bar of constant density  $\rho = \rho_0 = 1$  and monotonically increasing elastic modulus:

$$\mu(x) = 1 - (1 - \mu_1) \exp(-\gamma x), \quad x \geq 0, \tag{4.1}$$

where  $\mu_1 = \mu(0)$  and  $\gamma > 0$  is a constant. From (4.1) it follows that  $\mu_0$  is effectively unity, and thus, the velocity of wave propagation  $c_0 = (\mu_0/\rho_0)^{1/2} = 1$ .

We found that when we took the excitation  $\psi$  to be such as to produce a short pulse, we obtained very little reflection from  $x = L$  with any of the boundary conditions. Therefore, we chose the excitation to have the form

$$\psi(t) = \sin(2\pi\lambda t), \quad t > 0, \tag{4.2}$$

since this seems to us to yield a more severe test of the method. With this bar we perform a parametric study to examine the effect of various factors, including the type and position of the absorbing boundary, and frequency of excitation  $\lambda$ , on the accuracy of the results. The behavior for different values of  $\mu_1$  and  $\gamma$  was similar and only results for one combination,  $\mu_1 = 0.1$ , and  $\gamma = 0.588$ , are reported here. The corresponding values of  $\mu$ ,  $\alpha_{-1}$ ,  $\alpha_0$ ,  $\alpha_1$ , and  $\delta_{crit} = -\alpha_1/\alpha_0$  for different positions of the absorbing boundary are shown on Table I. Even when the value of  $\alpha_1$  is very small we found it to be quite destabilizing if not corrected by the introduction of  $\delta$ .

The solution within the domain of computation  $[0, L]$  is discretized with uniform piecewise linear finite elements of length  $h = 0.01$ . Only one mesh size is used in all the calculations in order to avoid the error inherent in the finite element discretization in our comparisons. For the time integration the mass matrix is chosen as the average of the lumped and consistent mass matrices. This combination, which we have discovered satisfies the global balance law

$$\frac{d}{dt} \int_{x_1}^{x_2} \rho u_t d\xi = \sigma(x_2, t) - \sigma(x_1, t) \quad \text{for any } x_1 < x_2. \tag{4.3}$$

yields more accurate results than either the lumped or consistent mass matrix by itself [6]. In calculating the element stiffness matrix we take the average value of

TABLE I  
Values of  $\mu$ ,  $\alpha_{-1}$ ,  $\alpha_0$ ,  $\alpha_1$ ,  $\delta_{crit}$  vs  $L$

$L$	$\mu$	$\alpha_{-1}$	$\alpha_0$	$\alpha_1$	$\delta_{crit}$
0.25	0.223	-0.472	-0.114	0.0297	0.260
0.50	0.329	-0.574	-0.099	0.0251	0.255
1.00	0.500	-0.707	-0.074	0.0191	0.260
8.00	0.992	-0.996	-0.001	0.0004	0.293

$\mu$  within each element. Even though no limitation need be imposed on the time step for stability, we have chosen  $\Delta t = 0.01$ , from accuracy considerations. This choice of  $h$  and  $\Delta t$  is based on a sensitivity study reported in [1].

To measure the accuracy of the approximation we will regard as an "exact" solution,  $u_{\text{ex}}^h$ , that obtained by placing the absorbing boundary at  $x = 8$ , for which  $c = (\mu/\rho)^{1/2}$  is sufficiently close to  $c_0$  that (2.2) can be used as the appropriate condition. In fact, numerical tests using (2.17a, b, c) and (2.28) at  $L = 8$  agreed with each other within five significant figures, with the solutions for any  $x$  becoming periodic with frequency  $\lambda$ , for large  $t$ . Keeping  $h$  and  $\Delta t$  fixed, the only difference between  $u^h$  and  $u_{\text{ex}}^h$  within  $[0, L]$  then will be due to the error introduced by the approximate boundary condition at  $x = L$ .

Figures 2 and 3 show the relative error in  $L_2$  of the displacement, for different types and positions of the absorbing boundary, for two frequencies of excitation. This error is defined by

$$\text{Relative error} = \left\{ \int_0^{0.25} (u_h - u_{\text{ex}}^h)^2 dx \right\}^{1/2} / \max_t \left\{ \int_0^{0.25} (u_{\text{ex}}^h)^2 dx \right\}^{1/2}. \quad (4.4)$$

(Other quantities, such as the displacement at the bar end showed similar errors.)

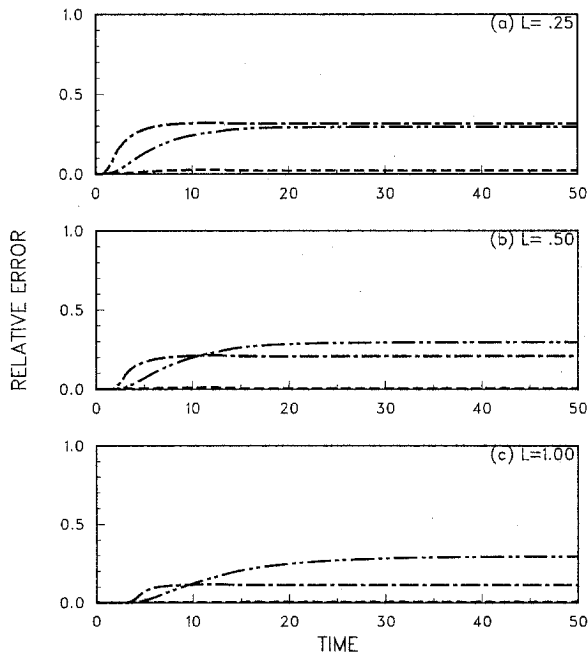


FIG. 2. Relative error in  $L_2$  of displacement vs time, for  $\lambda = 3$ , and three different types and positions of absorbing boundaries. ---, (2.22),  $N = -1$ ; - · - · -, (2.22),  $N = 0$ ; · · · ·, (2.28).

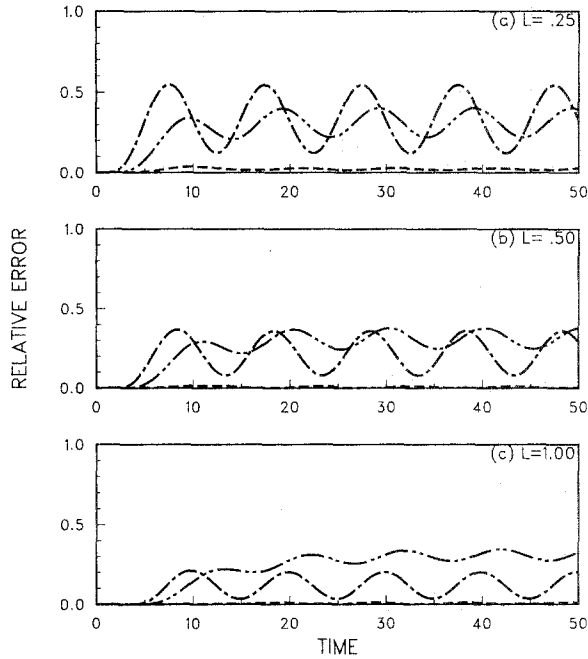


FIG. 3. Relative error in  $L_2$  for displacement vs time, for  $\lambda=0.1$ , and three different types and positions of absorbing boundaries. ---, (2.22),  $N = -1$ ; ----, (2.22),  $N = 0$ ; ····, (2.28).

The dotted-dashed and double dotted-dashed lines in Figs. 2 and 3 represent the errors corresponding to (2.22) and for  $N = -1, 0$  respectively. Clearly, the two solutions coincide until the first reflection from  $x = L$  reaches  $x = 0.25$ . While the two approximations introduce an error thereafter, this error remains stable over time. In contrast, the absolute error in  $L_2$  corresponding to (2.22) for  $N = 1$  (or, equivalently, (2.28) with  $\delta = 0$ ) with  $L = 0.25$  and  $\lambda = 3$ , exhibits a rapid growth with increasing time as shown by the solid line on Fig. 4. (The apparent reduction of the

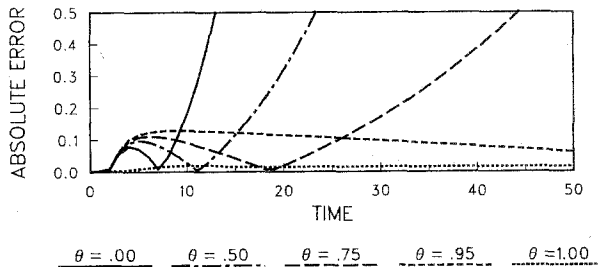


FIG. 4. Absolute error in  $L_2$  for displacement vs time, for the solution of (2.28) with  $\lambda = 3$  and  $L = 0.25$ ;  $\theta = \delta/\delta_{crit}$ .

error just before it begins to grow steadily is a consequence of plotting the error in absolute value. The actual error becomes negative as  $t$  increases.) Figure 4 also shows that introducing (2.28) for increasing values of  $\delta$ , as measured by  $\theta = \delta/\delta_{crit}$ , produces a decreasing rate of error growth. However, only when  $\delta$  attains the value  $\delta_{crit}$  does the error become stable. Taking  $\delta > \delta_{crit}$  also results in stable solutions of (2.28), but numerical experiments indicate that the accuracy deteriorates as  $\delta$  increases. (Results similar to those shown on Fig. 4 were obtained also for  $L = 0.5, 1$ ; and for  $\lambda = 0.1$ .)

The relative error in  $L_2$  corresponding to (2.28) with  $\delta = \delta_{crit}$  also is shown on Figs. 2 and 3, along with the results for (2.22) for  $N = -1$  and  $N = 0$ . The following trends are worthy of note in these figures:

All three approximate problems (2.22),  $N = -1, 0$  and (2.28) give good results for small  $t$ , with (2.22),  $N = 0$  showing some improvement over (2.22) with  $N = -1$ . For large  $t$  the performance of (2.28) is markedly better than (2.22),  $N = -1$  or 0. This is so even when the interval  $(0, L)$  is quite short. For  $L = 0.25\mu$  has increased only to 0.223, significantly less than its limit value  $\mu_0 = 1$ . With this short interval the relative error for (2.28) is less than 2% for all  $t$  values considered. This remarkable result represents a full order of magnitude of improvement over the performance of (2.22),  $N = -1, 0$ . (There may be other frequencies, however, for which the results become less accurate).

### 5. REMARKS ON TWO-DIMENSIONAL PROBLEMS

A two-dimensional version of the preceding problem occurs in the study of a special class of elastic waves (see [4]). We restrict ourselves here to homogeneous materials, which yields the two-dimensional wave equation.

Let  $\Gamma$  be a closed curve in the plane with exterior  $\Omega$ . We seek  $u(x, t)$  such that

$$\begin{aligned} u_{tt} &= \Delta u, & x \in \Omega, & & t > 0, \\ u_\nu &= f, & x \in \Gamma, & & t > 0 \quad (\nu \text{ exterior normal}), \\ u(x, 0) &\equiv u_t(x, 0) \equiv 0 & & & \text{in } \Omega. \end{aligned} \tag{5.1}$$

The solution should be outgoing.

We Laplace transform (5.1) in time and obtain

$$s^2 \hat{u} = \Delta \hat{u}, \quad x \in \Omega, \quad \hat{u}_\nu = \hat{f}, \quad x \in \Gamma. \tag{5.2}$$

Let  $\Gamma_1$  be a closed convex curve containing  $\Gamma$  in its interior and let  $\Omega_1$  be the exterior of  $\Gamma_1$  ( $\Gamma_1$  need not be a circle). We consider  $\hat{u}$  in  $\Omega_1$ . Let  $\hat{U}(x, s; t)$  be the solution of

$$s^2 \hat{U} = \Delta \hat{U}, \quad x \in \Omega_1, \quad U(x, s; t) = u(x, t), \quad x \in \Gamma_1. \tag{5.3}$$

Then one has

$$\hat{u}(x, s) = \int_0^\infty e^{-st} \hat{U}(x, s; t) dt, \tag{5.4}$$

$$\hat{u}_v(x, s)|_{\Gamma_1} = \int_0^\infty e^{-st} \hat{U}_v(x, s; t)|_{x \in \Gamma_1} dt. \tag{5.5}$$

Equation (5.5) represents an analog of formula (2.6).  $\hat{U}_v(x, s, t)|_{\Gamma_1}$  will be a linear functional of  $u(\cdot, t)$  on  $\Gamma_1$ ,  $\hat{U}_v(x, s; t) = \hat{\mathcal{F}}[u(\cdot, t)|_{\Gamma_1}](x, s)$ , hence (5.5) will yield

$$\hat{u}_v(x, s)|_{\Gamma_1} = \hat{\mathcal{F}}[\hat{u}(\cdot, s)](x, s). \tag{5.6}$$

Translation back to the time domain yields an analog of (2.7),

$$u_v(x, t)|_{\Gamma_1} = \mathcal{F}[u'(\cdot, \cdot)](x). \tag{5.7}$$

The operator  $\mathcal{F}$  in (5.7) is more complicated than that in (2.7). In (5.7) we have spatial non-locality on  $\Gamma_1$  as well as the time non-locality. Our procedure is to expand  $\hat{\mathcal{F}}$  for large  $s$  thus in effect reducing the time non-locality. It turns out that this procedure automatically reduces the spatial non-locality on  $\Gamma_1$ .

Our expansion for  $\hat{U}$  has the form

$$\hat{U}(x, s; t) \sim e^{-s\phi(x)} \sum_{k=0}^\infty U^k(x; t) s^{-k}, \tag{5.8}$$

$$\phi(x) = 0, \quad U^0(x; t) = u(x, t), \quad U^k(x, t) = 0, \quad k \geq 1, \quad x \in \Gamma_1.$$

We substitute (5.8) into (5.3) and equate coefficients of  $s^{-k}$ . This gives

$$\begin{aligned} |\text{grad } \phi|^2 &= 1, & 2 \text{ grad } \phi \cdot \text{grad } U^0 + \Delta \phi U^0 &= 0, \\ 2 \text{ grad } \phi \cdot \text{grad } U^k + \Delta \phi U^k &= \Delta U^{k-1}, & k &\geq 1. \end{aligned} \tag{5.9}$$

The calculations are facilitated by introducing a new coordinate system. Let  $\Gamma_1$  be  $x = X(\lambda)$ ,  $\lambda$  arc length, and let  $\mathbf{v}(\lambda)$  be the unit outer normal. Then the equation  $x = X(\lambda) + \tau \mathbf{v}(\lambda)$ ,  $\tau > 0$ , yields a coordinate system. Since  $\Gamma_1$  is convex this is global in  $\Omega_1$ . This coordinate system is orthogonal with form  $Q^2(d\lambda)^2 + (d\tau)^2$ ,  $Q = (1 - \tau\kappa(\lambda))$  where  $\kappa(\lambda)$  is the curvature. For any scalar field  $\chi$  one has

$$\begin{aligned} \text{grad } \chi &= \frac{1}{Q} \chi_\lambda X'(\lambda) + \chi_\tau \mathbf{v}, \\ \Delta \chi &= \frac{1}{Q} \frac{\partial}{\partial \lambda} \left( \frac{1}{Q} \chi_\lambda \right) + \frac{1}{Q} (Q \chi_\tau)_\tau. \end{aligned} \tag{5.10}$$

Using (5.10) one finds that (5.9) yields  $\phi = \tau$  and

$$\begin{aligned} 2U_\tau^0 + \frac{Q_\tau}{Q} U^0 &= 0, & U^0 &= u|_{\Gamma_1} & \text{at } \tau &= 0, \\ 2U_\tau^k + \frac{Q_\tau}{Q} U^k &= \Delta U^{k-1}, & U^k &= 0 & \text{at } \tau &= 0. \end{aligned}$$

Some elementary calculations yield the results

$$U_\tau^0|_{\Gamma_1} = \frac{1}{2} \kappa(\lambda) u|_{\Gamma_1}; \quad U_\tau^1 = \frac{1}{2} \frac{\partial^2}{\partial \lambda^2} u|_{\Gamma_1} + \frac{1}{8} \kappa^2 u|_{\Gamma_1}. \tag{5.11}$$

We observe that  $\partial/\partial v = \partial/\partial \tau$  and  $\phi_\tau = 1$ . Hence (5.8) yields

$$\hat{U}_v|_{\Gamma_1} \sim -sU^0|_{\Gamma_1} + \sum_{k=0}^\infty U_\tau^k|_{\Gamma_1} s^{-k} \tag{5.12}$$

and by (5.6),

$$\hat{u}_v(x, s)|_{\Gamma_1} = \hat{\mathcal{F}}[\hat{u}(\cdot, s)](x, s) = -su|_{\Gamma_1} + \sum_{k=0}^\infty \left( \int_0^\infty e^{-s\tau} U_\tau^k|_{\Gamma_1} d\tau \right) s^{-k}. \tag{5.13}$$

We construct approximate functionals  $\hat{\mathcal{F}}_n$  by truncating series (5.13) at  $n$ . This will give approximate boundary conditions to replace (5.6). Using (5.11) one can check that the first three are

$$\begin{aligned} n = -1: & \quad u_v|_{\Gamma_1} = -u_t|_{\Gamma_1}, \\ n = 0: & \quad u_v|_{\Gamma_1} = -u_t|_{\Gamma_1} + \frac{1}{2} \kappa u|_{\Gamma_1}, \\ n = 1: & \quad u_{v\tau}|_{\Gamma_1} = -u_{tt}|_{\Gamma_1} + \frac{1}{2} \kappa u_t|_{\Gamma_1} + \frac{1}{2} \frac{\partial^2}{\partial \lambda^2} u|_{\Gamma_1} + \frac{1}{8} \kappa^2 u|_{\Gamma_1}. \end{aligned} \tag{5.14}$$

Notice that the  $n = -1$  and  $n = 0$  cases are completely local in space while the spatial non-locality in  $n = 1$  is only the second tangential derivative.

When the Kreiss well-posedness theory is applied to the present situation one considers the case of a half-space so that one can assume  $\kappa = 0$ . In this case all three of the conditions (5.14) give well-posed problems in the sense of Kreiss. Once again, however, there is a stronger dissipativity condition which would prevent exponential error growth. We show that for a curve,  $\kappa \neq 0$ , the case  $n = 1$  in (5.14) need not be dissipative.



The energy integral arguments of Section 2 can be repeated to yield the following results. We start with the analog of (2.24):

$$\begin{aligned} s^2 \hat{u} &= A \hat{u} && \text{in } \Omega_1, \\ \hat{u}_v &= 0 && \text{on } \Gamma, \quad \hat{u}_v|_{\Gamma_1} = \mathcal{G}[\hat{u}|_{\Gamma_1}] \end{aligned} \tag{5.15}$$

where  $\mathcal{G}$  is a spatial functional. The condition of dissipativity is again that (5.15) have no non-zero solutions in  $\Re s \geq 0$ . There is also an analog of conditions  $(\hat{R})$  and  $(\hat{I})$ , namely,

$$\begin{aligned} \int_{\Gamma_1} \mathcal{G}[\hat{\phi}(\cdot)](x, \xi) \bar{\phi}(x) d\lambda &< 0 && \text{for } s = \xi > 0, && (\hat{R}) \\ \Im \int_{\Gamma_1} \mathcal{G}[\hat{\phi}(\cdot)](x, \xi + i\eta) \bar{\phi}(x) d\lambda &\begin{cases} < 0 \\ > 0 \end{cases} && \text{for } \begin{cases} \xi \geq 0, & \eta > 0, \\ & \eta < 0. \end{cases} && (\hat{I}) \end{aligned}$$

One can again show that the functional  $\mathcal{F}$  in (5.7) for the exact solution satisfies  $(\hat{R})$  and  $(\hat{I})$ . Further  $\hat{R}$  and  $\hat{I}$  together imply that  $\mathcal{G}$  is dissipative. Finally one can show that if one solves (5.1) for  $u$  and the problem with the modified functional  $\mathcal{G}$  on  $\Gamma_1$  for  $U$  then  $u - U$  will remain bounded if  $\mathcal{G}$  is dissipative but will grow exponentially if  $\mathcal{G}$  is not dissipative.

It is easily checked that the functionals  $\mathcal{F}_{-1}$  and  $\mathcal{F}_0$  satisfy  $(\hat{R})$  and  $(\hat{I})$  ( $\kappa$  is negative). For  $n = 1$  we have

$$\begin{aligned} &\int_{\Gamma_1} \mathcal{F}_1[\hat{\phi}(\cdot)](x, \xi) \bar{\phi}(\lambda) d\lambda \\ &= -s \int_{\Gamma_1} |\hat{\phi}|^2 d\lambda + \frac{1}{2} \int_{\Gamma_1} \kappa |\hat{\phi}|^2 d\lambda \\ &\quad - \left\{ \frac{1}{2} \int_{\Gamma_1} |\hat{\phi}'|^2 d\lambda - \frac{1}{8} \int_{\Gamma_1} \kappa^2 |\hat{\phi}|^2 d\lambda \right\} \frac{1}{s}. \end{aligned} \tag{5.16}$$

We see from (5.16) that  $\mathcal{F}_1$  will satisfy  $(\hat{R})$  if the coefficient of  $s^{-1}$  is negative. When  $\kappa \neq 0$  this need not be true. We can, however, restore condition  $(\hat{R})$ , just as we did in Section 2, for a convex  $\Gamma_1$ . Suppose  $0 > \bar{\kappa} \geq \kappa \geq \underline{\kappa}$ . Then if we introduce a new  $\mathcal{F}_1$  by replacing  $s^{-1}$  by  $(s + \delta)^{-1}$  for  $\delta > -\bar{\kappa}^2/4\underline{\kappa}$  it is easy to verify that this new  $\mathcal{F}_1$  will satisfy  $(\hat{R})$ . This replaces the third condition in (5.14) by

$$u_{vt} + \delta u_v = -u_{tt} + (\frac{1}{2}\kappa - \delta) u_t + \frac{1}{2}u_{\lambda\lambda} + (\frac{1}{8}\kappa^2 + \frac{1}{2}\kappa\delta) u \quad \text{on } \Gamma_1. \tag{5.17}$$

Condition  $(\hat{I})$  is different. It would be satisfied if the coefficient of  $s^{-1}$  in (5.16) were positive which is almost certainly not true. Moreover, it cannot be restored by

replacing  $s^{-1}$  by  $(s + \delta)^{-1}$  since  $\int_{\Gamma_1} |\hat{\phi}'|^2 d\lambda$  cannot be dominated by  $\int_{\Gamma_1} |\hat{\phi}|^2 d\lambda$ . We hope that good results will be obtained by choosing  $\delta$  to ensure  $(\hat{R})$  above. If this is not so we do have a suggestion to deal with  $(\hat{I})$ . Let us introduce this while simultaneously describing a proposed numerical scheme.

Consider the problem of solving  $u_{tt} = \Delta u$  in the region  $\Omega_2$  between  $\Gamma$  and  $\Gamma_1$  with  $u_v = f$  on  $\Gamma$  and (5.17) on  $\Gamma_1$ . If we introduce  $\tau = u_v|_{\Gamma_1}$  as an auxiliary variable then a variational formulation is to find  $(u, \tau)$  such that

$$\begin{aligned} \int_{\Omega_2} u_{tt} v \, dx + \int_{\Omega_2} \nabla u \cdot \nabla v \, dx - \int_{\Gamma_1} \tau v \, d\lambda &= \int_{\Gamma} f v \, d\lambda, \\ \int_{\Gamma_1} (\tau_t + \delta \tau) \mu \, d\lambda + \int_{\Gamma_1} (u_{tt} - (\tfrac{1}{2}\kappa - \delta) u_t & \\ - (\tfrac{1}{8}\kappa^2 + \tfrac{1}{2}\kappa\delta) u) \mu \, d\lambda + \tfrac{1}{2} \int_{\Gamma_1} u_\lambda \mu' \, d\lambda &= 0, \end{aligned} \tag{5.18}$$

for all pairs  $(v, \mu)$ . To implement this one could introduce the finite-dimensional spaces  $S^h$  and  $A^h$  on  $\Omega_1$  and  $\Gamma_1$  and then find  $u^h \in S^h, \tau^h \in A^h$  so that (5.18) holds for any  $v^h \in S^h, \mu^h \in A^h$ .

We have already indicated that  $\delta$  can be chosen so that  $(\hat{R})$  is satisfied. Our observation concerning  $(\hat{I})$  is that once the space  $A^h$  is fixed one can choose a  $\delta = \delta_h$  so that condition  $(\hat{I})$  is satisfied for all  $\varphi \in A^h$ . Suppose, for instance, that  $A^h$  is chosen as the space of linear functions on  $\Gamma_1$  with mesh size  $h$ . Thus if  $\lambda_j, j = 1, \dots, N^h$ , are parameter points,  $A^h = \langle \zeta_1^h, \dots, \zeta_{N^h}^h \rangle$  where  $\zeta_j^h$  are piecewise linear with  $\zeta_j^h(\lambda_k) = \delta_{jk}$ . Then  $\varphi \in A^h$  means  $\varphi(\lambda) = \sum_1^{N^h} \varphi_j \zeta_j(\lambda), \varphi'(\lambda) = \sum_1^{N^h} \varphi_j \zeta_j'(\lambda)$ . If we put  $\boldsymbol{\varphi} = (\varphi_1, \dots, \varphi_{N^h})$  then there is a positive definite matrix  $\mathbf{J}^h$  and a non-negative matrix  $\mathbf{L}^h$  such that for any  $\boldsymbol{\varphi} \in A^h$

$$\int_{\Gamma_1} \varphi(\lambda)^2 \, d\lambda = (\boldsymbol{\varphi}, \mathbf{J}^h \boldsymbol{\varphi}), \quad \int_{\Gamma_1} \varphi'(\lambda)^2 \, d\lambda = (\boldsymbol{\varphi}, \mathbf{L}^h \boldsymbol{\varphi}).$$

It follows that for some  $\alpha > 0$

$$\int_{\Gamma_1} \varphi'(\lambda)^2 \, d\lambda \leq \| \mathbf{L}^h \| \| \boldsymbol{\varphi} \|^2 \leq \alpha \| \mathbf{L}^h \| \int_{\Gamma_1} \varphi^2(\lambda) \, d\lambda. \tag{5.19}$$

It is not difficult to show with this inequality that, for  $h$  fixed, then replacing  $s^{-1}$  by  $(s + \delta_h)^{-1}$  in the right side of (5.16) with  $\delta_h$  sufficiently large ensures that  $(\hat{I})$  is satisfied on  $A^h$ . This will at least guarantee that the solutions of (5.18) do not grow exponentially if  $f$  is suitably restricted. We note, however, that  $\| \mathbf{L}^h \|$  is of order  $h^{-2}$ ; hence the required  $\delta_h$  grows as  $h$  decreases.

*Remark 1.* We want to compare our ideas with those of Engquist and Majda. In [4] these authors treat our problem for the special case of a half-space, that is,

$$u_{tt} = u_{xx} + u_{yy} \quad \text{in } x > 0$$

with  $\Gamma: x = 0$ . Then they choose for  $\Gamma_1$  a line  $x = L$ . In this case the calculation of  $\mathcal{F}$  in (5.6) is facilitated by taking a Fourier transform with respect to  $y$ . If  $\tilde{u}(x, s, \omega)$  is the transform with respect to  $t$  and  $y$  then they find

$$\tilde{u}_x(L, s, \omega) = (s^2 - \omega^2)^{1/2} \tilde{u}(L, s, \omega). \tag{5.20}$$

Their procedure is to expand  $(s^2 - \omega^2)^{1/2}$  by using Padé approximations and then translate the results back to  $t, x, y$  space, thus obtaining a sequence of approximate problems. For  $n = -1, 0$ , and  $1$  our results in (5.14), with  $\kappa \equiv 0$ , agree with theirs. In [4] they consider a more general  $\Gamma$  but take  $\Gamma_1$  to be a circle. Again our results for  $n = -1, 0$  and  $1$  agree with theirs. It is not clear how they would proceed to get higher order terms in this case.

If we were to continue our process in the half-space case, our results would not agree with those in [4]. In fact what we would get would be the result of expanding  $(s^2 - \omega^2)^{1/2}$  using Taylor series and as Engquist and Majda point out these lead to ill-posed problems. We do not know if the device indicated in Section 2 for higher order approximations can be used to stabilize the higher order results here, at least on the finite element spaces.

*Remark 2.* For the special case in which  $\Gamma_1$  is a circle our results can also be compared to those of Bayliss and Turkel [2]. The procedure in [2] is obtained by using a far-field expansion from scattering theory and is designed to produce a sequence of approximate boundary conditions having the property that they differ from the exact condition by a term which is  $O(R^{-n-1})$ ,  $R$  the radius of  $\Gamma_1$ . It is not difficult to see that, for a circle, our procedure has the property that the  $k$ th term in (5.13) is  $O(R^{-k})$  so it has the same property as that in [2]. This means that for any approximation  $\mathcal{F}_n$  with  $n \geq 1$  one can expect to make the errors go to zero by choosing  $R$  large, but, without some modification, not uniformly in time.

The authors thank the referees for a number of very helpful suggestions.

REFERENCES

1. A. BARRY, M. S. thesis, Carnegie Mellon University, Pittsburgh, PA, 1986 (unpublished).
2. A. BAYLISS AND E. TURKEL, *Commun. Pure Appl. Math.* **33**, 707 (1980).
3. R. COURANT AND D. HILBERT, *Methods of Mathematical Physics*, Vol. II (Interscience, New York, 1962), p. 640.

4. B. ENGQUIST AND A. MAJDA, *Math. Comput.* **31**, 629 (1977).
5. B. ENGQUIST AND A. MAJDA, *Commun. Pure Appl. Math.* **32**, 313 (1979).
6. G. L. GOUDREAU AND A. L. TAYLOR, *Comput. Methods Appl. Mech. Eng.* **2**, 69 (1972).
7. B. GUSTAFFSON AND H.-O. KREISS, *J. Comput. Phys.* **30**, 333 (1979).
8. T. M. HAGSTROM, PH. D. THESIS, California Institute of Technology, Pasadena, California, 1983 (unpublished).
9. R. L. HIGDON, *Math. Comput.* **49**, 65 (1987).
10. H.-O. KREISS, *Commun. Pure Appl. Math.* **33**, 277 (1970).
11. E. TURKEL, *Comput. Fluids* **11**, 120 (1983).